Nov 9th, 12:00 AM - 12:00 AM

On the Direct Strength Design of Cold-Formed Steel Columns Falling in Local-Distortional Interactive Modes

André Dias Martins

Dinar Camotim

Pedro Borges Dinis

Wei-Wen Yu International Specialty Conference on Cold-Formed Steel Structures
Baltimore, Maryland, U.S.A, November 9 & 10, 2016

On the Direct Strength Design of Cold-Formed Steel Columns Failing in Local-Distortional Interactive Modes

André Dias Martins[1], Dinar Camotim[1] and Pedro Borges Dinis[1]

Abstract

This paper present and discusses proposals for the codification of efficient design approaches for cold-formed steel columns affected by local-distortional (L-D) interaction. These proposals, based on the Direct Strength Method (DSM), were developed, calibrated and validated on the basis of experimental and numerical (shell finite element) failure load data concerning columns with several cross-section shapes and obtained from investigations carried out by various researchers. Three types of L-D interaction are taken into account, namely "true L-D interaction", "secondary local bifurcation L-D interaction" and "secondary distortional bifurcation L-D interaction". Moreover, previously available DSM-based design approaches to handle column L-D interactive failures are reviewed and their merits are assessed and compared with those exhibited by the present proposals. The paper also presents reliability assessments of the failure load predictions provided by the available and proposed DSM-based design approaches, following the procedure prescribed by the current version of the North American Specification (NAS) for the Design of Cold-Formed Steel Structures (AISI 2012).

1. Introduction

Cold-formed steel (CFS) members invariably display very slender thin-walled open cross-sections, a feature responsible for their high susceptibility to several individual (local – L, distortional – D, global – G) or coupled buckling phenomena (L-G, L-D, D-G, L-D-G). Nowadays, it is consensual amongst the technical and scientific communities working with CFS structures that it is necessary to establish efficient (safe and accurate) design approaches to handle interactive failures, a goal that has long been achieved for L-G interaction, a coupling phenomenon affecting both cold-formed and hot-rolled steel members. In the case of CFS members, design approaches based on the "Effective Width" and "Direct Strength" concepts are currently codified. Concerning interactive

[1] CERIS, ICIST, DECivil, Instituto Superior Técnico, Universidade de Lisboa, Av. Rovisco Pais, 1049-001 Lisboa, Portugal.

failures involving distortional buckling, virtually exclusive of CFS members, the situation is completely different and adequate design approaches can only be established after in-depth knowledge about the structural response of members affected by the coupling phenomenon under consideration has been acquired. In the case of CFS columns undergoing L-D interaction, such knowledge already exists, mainly due to the efforts of the authors. Moreover, design approaches based on the Direct Strength Method (DSM – Schafer 2008) have been proposed to predict specifically L-D interactive failures in columns exhibiting most of the cross-section shapes of practical interest – the estimates provided by such design approaches were shown to be safe and reliable. Thus, it may be rightfully argued that only the codification of DSM-based design approaches against column L-D interactive failures is missing – indeed, the currently codified DSM column design curves concern only L, D, G and L-G (interactive) collapses, *i.e*, the column nominal strength is given by $P_n=min\{P_{nL}, P_{nD}, P_{nG}, P_{nLG}\}$[2]. The aim of this work is to propose additional design approaches, so that $P_n=min\{P_{nL}, P_{nD}, P_{nG}, P_{nLG}, P_{nLD}\}$.

As mentioned in the previous paragraph, the objective of this paper is to present and discuss proposals for the codification of efficient DSM-based design approaches for CFS columns experiencing L-D interaction. These proposals were developed, calibrated and validated on the basis of (i) experimental failure loads obtained from test campaigns carried out be several researchers (the authors were involved in some of them), and (ii) extensive numerical failure load data obtained from shell finite element (SFE) materially and geometrically non-linear imperfect analyses (GMNIA). The above experimental and numerical failure loads concern columns with various cross-section shapes, namely plain, web-stiffened and web/flange-stiffened lipped channels, hat-sections, zed-sections and rack-sections – hereafter termed "C", "WSLC", "WFSLC", "H", "Z", "R" –, *i.e.*, those displayed in Fig. 1)[3]. Moreover, three types of L-D interaction are taken into account, namely (i) "true L-D interaction" (TI), occurring for columns with close local and distortional critical buckling loads (strongest L-D interaction effects), (ii) "secondary local bifurcation L-D interaction" (SLI) and (iii) "secondary distortional bifurcation L-D interaction" (SDI) – the last two occur for columns with the non-critical buckling load visibly above the critical one, but significantly below the squash load. Since the SLI was found to cause only negligible failure load erosion (with respect to the distortional ultimate strength), the corresponding column failures can be deemed adequately covered by the currently codified DSM column distortional design curve. However, the remaining two L-D interaction types must be addressed, *i.e.*, specific design approaches have to be established to handle the corresponding column interactive failures. While the authors believe that, on the basis of the existing knowledge, the codification of an efficient design approach for columns undergoing TI constitutes a fairly straightforward task, attaining the same goal for columns experiencing SDI still poses a few challenging problems, namely those dealing with the identification of a "border" beyond which L-D interaction is

[2] The values of P_{nL} and P_{nLG} are obtained from the same set of expressions.

[3] It is worth noting that, currently, the WFSLC are not "pre-qualified column cross-sections".

no longer relevant. Moreover, some previously available DSM-based design approaches for columns failing in L-D interactive modes are reviewed, and their merits are assessed and compared with those exhibited by the proposed ones[4]. Finally, the paper also presents reliability assessments of the failure load predictions provided by the proposed DSM-based design approaches, following the procedure prescribed by the North American Specification (NAS) for the Design of Cold-Formed Steel Structures (AISI 2012).

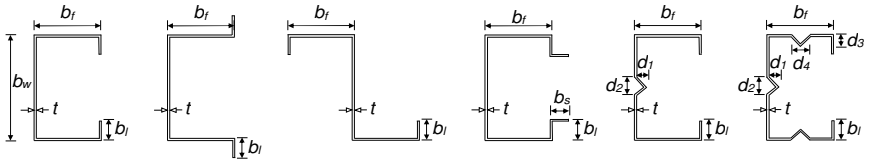

Fig. 1. CFS cross-section dimensions of the columns analyzed: (a) lipped channel, (b) hat-section, (c) zed-section, (d) rack-section, (e) web-stiffened lipped channel and (f) web-flange-stiffened lipped channel

2. Database of Failure Loads of CFS Columns Experiencing L-D Interaction

2.1 Experimental Failure Loads

Although there exist a few test campaigns reported in the literature that were carried out with the specific aim of investigating L-D interaction in fixed-ended CFS columns, exhibiting both plain and stiffened lipped cross-sections, the specimens providing clear experimental evidence of this coupling phenomenon and ensuing failure load erosion are relatively scarce – certainly, much less than those collected to propose/calibrate the existing L, D, G and L-G DSM design curves/expressions approaches (Schafer 2008). Indeed, the available experimental results evidencing the occurrence of L-D interaction in fixed-ended CFS columns are due to (i) Kwon and Hancock (1992), Young & Rasmussen (1998), Kwon *et al.* (2009), Loughlan *et al.* (2012) and Young *et al*. (2013), for C columns, (ii) Kwon *et al.* (2005), for C and H columns, (iii) Dinis *et al*. (2014a), for R columns, (iv) Kwon & Hancock (1992), Kwon *et al.* (2009), Yap & Hancock (2011) and He *et al*. (2014), for WSLC columns, (v) Yang & Hancock (2004), for WFSLC columns, and (vi) Yap & Hancock (2008), for columns with complex-stiffened cross-sections[5] – no Z column test results were found in the literature.

Table 1 summarises the available test results concerning fixed-ended CFS experiencing L-D interaction[6]. The reported/measured geometrical and material properties were used to evaluate the column squash and critical local/distortional/global buckling loads, the

[4] Due to space limitations, not all the available DSM-based design approaches are reviewed here.

[5] Due to the unusual cross-section shapes, and also the small number of test results reported by Yap & Hancock (2008), it was decided to exclude them from this study.

[6] Note that another test campaign involving CFS lipped channel columns was recently reported by Dinis *et al*. (2014b). However, these results were excluded from this study due to the fact that no clear L-D failures were observed. Indeed, the specimens tested, which were originally designed to fail in D-G interactive modes, exhibited only either D or L-D-G interactive failures (due to poor manufacture).

latter by means of the GBTUL code (Bebiano *et al*. 2008), based on Generalized Beam Theory (GBT) – in some cases (*e.g.*, Yap & Hancock 2008, 2011, and He *et al*. 2014) discrepancies were found between the values obtained and those reported (specially the distortional buckling loads). Based on these values, the above test results were divided into six sets, according to the specimen (i) cross-section shape (plain, web-stiffened and web/flange-stiffened lipped channel cross-sections – PCS, comprising C, H, R – WSLC and WFSLC) and (ii) L-D interaction nature (SLI, TI or SDI) – the number of specimens tested are given between brackets in Table 1. The L-D interaction nature was determined as reported by the authors (Martins *et al*. 2015a): (i) TI if $0.8 \leq P_{crD}/P_{crL} \leq 1.3$ (regardless of the yield stress value), (i) SLI[7] if $P_{crD}/P_{crL} < 0.8$ and (iii) SDI if $P_{crD}/P_{crL} > 1.3$.

The observation of Table 1 shows that reasonably sized numbers of test results exist only for (i) PCS columns affected by SDI (54 tests) and (ii) WSLC columns experiencing TI (30 tests) – for the remaining cases, the numbers of test results are scarce or even null. A total of 120 test results were collected, a number that, naturally, is considerably below the number of tests considered to develop/calibrate the currently codified DSM local (P_{nL}) and distortional (P_{nD}) column strength curves (249 tests – see Schafer 2008).

Table 1. Available test results concerning CFS columns experiencing L-D interaction

	SLI	**TI**	**SDI**
PCS	Kwon & Hancock (1992) [1]	Kwon & Hancock (1992) [4] Kwon *et al*. (2005) [5]	Young *et al*. (2013) [16] Loughlan *et al.* (2012) [20] Young & Rasmussen (1998) [3] Kwon *et al.* (2009) [5] Dinis *et al.* (2014a) [10]
WSLC	Kwon & Hancock (1992) [3] Yap & Hancock (2011) [5]	Kwon & Hancock (1992) [3] Kwon *et al.* (2009) [7] He *et al.* (2014) [14] Yap & Hancock (2011) [6]	Kwon *et al.* (2009) [3] He *et al.* (2014) [3]
WFSLC		Yang & Hancock (2004) [8]	Yang & Hancock (2004) [4]
	9	47	64

2.2 Numerical Failure Loads

Extensive parametric studies, consisting of ABAQUS (Simulia 2008) SFE GMNIA, were conducted in the last few years to complement the experimental failure load database given in Table 1 with numerical failure load data. Due to space limitations, the modelling issues involved in the above studies are not addressed here – they can be found, *e.g.*, in Silvestre *et al*. (2012). The columns analyzed were (i) C columns with $0.9 \leq P_{crD}/P_{crL} \leq 1.0$ (TI), reported by Silvestre *et al*. (2012), and with $0.4 \leq P_{crD}/P_{crL} \leq 2.4$ (SLI, TI, SDI), reported by Martins *et al*. (2015a), (ii) H, Z and R columns with $0.9 \leq P_{crD}/P_{crL} \leq 1.0$ (TI), reported by Dinis & Camotim (2015), and with $0.4 \leq P_{crD}/P_{crL} \leq 2.4$ (SLI, TI, SDI), reported by Martins *et al*. (2015a), (iii) WSLC columns $0.4 \leq P_{crD}/P_{crL} \leq 2.4$ (SLI, TI, SDI),

[7] In this type of L-D interaction, the identification of the "border" between pure distortional collapses and L-D interactive ones (stemming from SLI and occurring for "high enough yield stresses") is only of academic interest, due to the negligible failure load erosion (with respect to the pure distortional failure loads).

reported by Martins *et al.* (2016a), and (iv) WFSLC columns $0.4 \leq P_{crD}/P_{crL} \leq 2.0$ (SLI, TI, SDI), reported by Martins *et al.* (2015b, 2016b), totalling over 2000 results. Since all the numerical failure load data were obtained for columns containing critical-mode initial geometrical imperfections (IGI) with small amplitudes (10% of the wall thickness t), an imperfection sensitivity study is carried out next, in order to assess the influence of the initial imperfection amplitude on the column failure load.

Although there are no definitive guidelines concerning what IGI type and amplitude should be included in SFE GMNIA of CFS members, most researchers usually adopt the statistical approach developed by Schafer & Peköz (1998), which is also followed here. Therefore, two different IGI types/shapes are considered: local and distortional (Types I and II, in the nomenclature of Schafer and Peköz (1998)), akin to the corresponding two critical buckling modes. Four initial imperfections amplitudes were considered for each of them, namely (i) $0.1t$ (value adopted in all the previous numerical simulations), and (ii) values corresponding to a given probability (P) that a random imperfection amplitude (Δ) is below a given one (δ), *i.e.*, $P(\Delta<\delta)$ − the probabilities considered were 25%, 50%, 75%, leading to $0.14t$, $0.34t$, $0.66t$ (Type I), and $0.64t$, $0.94t$, $1.55t$ (Type II).

The imperfection sensitivity study concerns C columns with b_w=120, b_f=110, b_l=10, t=1.4 and L=900mm (see Fig. 1), for which $P_{crD} \approx P_{crL}$. Figs. 2(a)-(b) plot, against λ_L and λ_D ($\equiv\lambda$), the P_U/P_y (failure-to-squash load) ratios of columns containing Type I and Type II IGI, respectively. The observation of these figures shows that:

(i) For both Type I and Type II IGI, the ultimate strength of the columns exhibiting moderate-to-high slenderness (λ>1.25), *i.e.*, those predominantly governed by the geometrically non-linear effects, is virtual insensitive to the IGI amplitude.

(ii) On the other hand, the stocky columns ($\lambda \leq 1.25$) are, naturally, strongly affected by the IGI amplitude − the influence is most relevant for the Type I IGI (see Fig. 2(a)).

(iii) The IGI amplitude adopted in the previous studies ($0.1t$) may be deemed adequate, since (iii_1) the most detrimental IGI shape was found to be the distortional one (in the context of columns experiencing TI − Silvestre *et al.* 2012, Dinis & Camotim 2015), (iii_2) the number of columns with $\lambda \leq 1.25$ that exhibit failure load erosion due to L-D

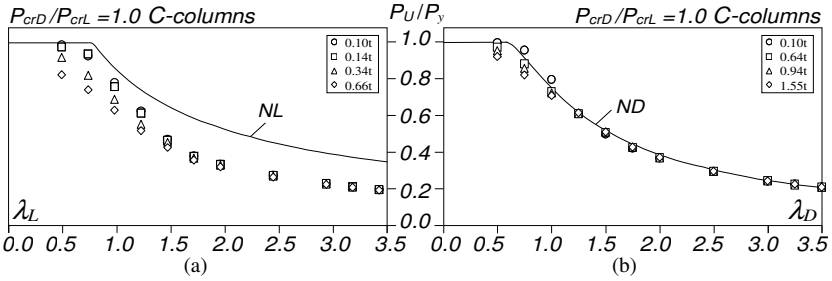

Fig. 2. Imperfection sensitivity study: (a) local (Type I) and (b) distortional (Type II) initial imperfections

interaction is rather small, and (iii$_3$) the additional local IGI shape adopted by Martins *et al*. (2015a,b,2016a,b) when analyzing columns with $P_{crD}>P_{crL}$ (SDI), was shown to erode only the failure loads of columns exhibiting moderate-to-high λ_L values.

3. DSM-Based Approaches to Handle Columns for L-D Interactive Failures

Several DSM-based approaches intended to handle CFS column L-D interactive failures have been proposed in the relatively recent past. Indeed, almost all the authors appearing in Table 1 either proposed new design expressions or suggested modifications of the existing ones. However, the more consensual for the CFS technical/scientific community are due to Schafer (2002): the NLD and NDL approaches, both based on the currently codified local (P_{nL})[8] and distortional (P_{nD}) strength curves. The corresponding "Winter-type" expressions are obtained by replacing P_y by either (i) P_{nD} in the P_{nL} equations (NLD approach – P_{nLD}) or (ii) P_{nL} in the P_{nD} equations (NDL approach – P_{nDL}), and read

$$P_{nDL} = \begin{cases} P_{nL} & , \quad \lambda_{DL} \le 0.561 \\ P_{nL}\lambda_{DL}^{-1.2}(1-0.25\lambda_{DL}^{-1.2}), & \lambda_{DL} > 0.561 \end{cases} \tag{1}$$

$$P_{nLD} = \begin{cases} P_{nD} & , \quad \lambda_{LD} \le 0.776 \\ P_{nD}\lambda_{LD}^{-0.8}(1-0.15\lambda_{LD}^{-0.8}), & \lambda_{LD} > 0.776 \end{cases} \tag{2}$$

where $\lambda_{DL}=(P_{nL}/P_{crD})^{0.5}$ and $\lambda_{LD}=(P_{nD}/P_{crL})^{0.5}$ are the distortional (local) slenderness based on the local (distortional) strength. Since the NDL and NLD approaches yield similar results, and due to space limitations, only the former is kept in the remainder of this work.

The three types of L-D interaction are addressed separately in the next sections: first TI ($0.8\le P_{crD}/P_{crL}\le 1.3$), then SDI ($P_{crD}/P_{crL}>1.3$) and, finally, SLI ($P_{crD}/P_{crL}<0.8$) − this order is associated with a decreasing failure load erosion due to L-D interaction. Several design approaches are considered for each type of L-D interaction and their merits are assessed though the evaluation of the LRFD (Load and Resistance Factor Design) resistance factor (ϕ) prescribed by the North American Specification (NAS) for Cold-Formed Steel Structures (AISI 2012 − Section F.1.1), which is given by

$$\phi = C_\phi M_m F_m P_m e^{-\beta_o \sqrt{V_M^2 + V_F^2 + C_P V_P^2 + V_Q^2}} \tag{3}$$

where C_ϕ=1.52 (calibration coefficient for LRFD), M_m=1.10 and F_m=1.00 (taken from Table F1 of AISI 2012) are the material and fabrication factor mean values, β_0 is the target reliability value (β_0=2.5 for structural members in LRFD), V_M=0.10, V_F=0.05 and V_Q=0.21 (again taken from Table F1 of AISI 2012) are the material factor, fabrication factor and load effect coefficients of variation, respectively, and C_p is a correction factor

[8] The currently codified P_{nL} curve is intended for the design against pure local and local-global interactive failures – in fact, it may be said that it is a P_{nLG} curve. In this work the pure P_{nL} curve is considered – it is obtained from the currently codified one (AISI 2012) by replacing P_{nG} with P_y.

dependent on the number of tests. P_m and V_p are the mean and standard deviation of the "exact"-to-predicted failure load ratios. The value recommended for members under compression is ϕ=0.85, regardless of the failure mode nature (L, D, G or interactive).

3.1 True L-D Interaction (TI)

The "generalized modified NDL approach" (MNDL) has been successfully used by the authors to predict failure loads of C, H, Z, R, WSLC, WFSLC columns undergoing TI. Initially developed by Silvestre *et al*. (2012), in the context of C columns, it was later extended (i) to H, Z, R columns, by Dinis & Camotim (2015), and also (ii) to WSLC, WFSLC columns, by the authors (Martins *et al*. 2015b, 2016a,b). This design approach[9] is based on the definition of a modified local strength P^*_{nL}, dependent on the column critical half-wave length ratio L_{crD}/L_{crL} (obtained from simply supported column signature curves), and estimates the column failure loads by replacing P_{NL} with P^*_{NL} in the NDL equations (1) – this modified local strength leads to P_{nD} and P_{nDL} estimates, respectively for $L_{crD}/L_{crL} \leq a$ and $L_{crD}/L_{crL} \geq b$ – see the graphical illustration in Fig. 3(a). The integers "a" and "b" vary with the cross-section shape: (i) a=4 and b=8 (C, H, Z, R), (ii) a=8 and b=12 (WSLC) and (iii) a=14 and b=40 (WFSLC). The P_{MnDL} approach is given by

$$P_{MnDL} = \begin{cases} P^*_{nL} & , \quad \lambda^*_{DL} \leq 0.561 \\ P^*_{nL}\ \lambda^{*\ -1.2}_{DL}\ (1-0.25\lambda^{*\ -1.2}_{DL}), & \lambda^*_{DL} > 0.561 \end{cases} \tag{4}$$

with

$$P^*_{nL} = \begin{cases} P_y & , \quad \dfrac{L_{crD}}{L_{crL}} \leq a \\ P_y + \left(\dfrac{a}{b-a} - \dfrac{1}{b-a}\dfrac{L_{crD}}{L_{crL}} \right)\left(P_y - P_{nL}\right), & a \leq \dfrac{L_{crD}}{L_{crL}} \leq b \\ P_{nL} & , \quad \dfrac{L_{crD}}{L_{crL}} \geq b \end{cases} \tag{5}$$

where $\lambda^*_{DL}=(P^*_{nL}/P_{crD})^{0.5}$ denotes the distortional slenderness based on the modified local strength P^*_{nL}.

Figs. 4(a)-(b) plot the P_{Exp}/P_{nDL} and P_{Exp}/P_{MnDL} ratios against λ_D for all the available experimental results concerning columns undergoing TI (see Table 1). On the other hand, Figs. 5(a)-(f) and 6(a)-(f) plot the P_U/P_{MnDL} and P_U/P_{nDL} ratios against λ_D for the numerical failure loads obtained by the authors – the values concerning the C, H, Z, R, WSLC, WFSLC columns are plotted separately. Finally, Tables 2 and 3 show the n (number of failure loads), P_m, V_p and ϕ values concerning the NDL and MNDL estimates of the (i) experimental and (ii) numerical failure loads. The observation of all these results leads to the following comments:

---

[9] Originally, this design approach adopted P_{nD} for stocky columns (λ_D<1.5). However, in view of the imperfection sensitivity study presented in Section 2.2, this condition was not longer adopted in this work.

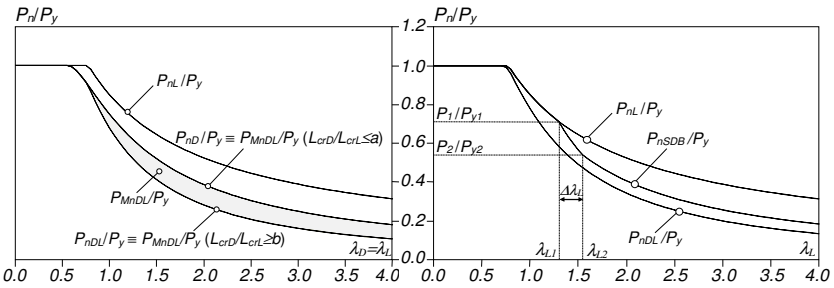

Fig. 3. Strength curves associated with the (a) generalized MNDL (P_{MnDL}/P_y vs. $\lambda_D \equiv \lambda_L$) and (b) NSDB ($P_{nSDB}/P_y$ vs. λ_L) design approaches

(i) Figs. 4(a)-(b) show that the NDL approach outperforms its MNDL counterpart in predicting the experimental failure loads: mean values and standard derivation equal to (i_1) 1.04 and 0.18, and (i_2) 0.88 and 0.10, respectively. This assertion is also corroborated by the resistance factors given in Table 2: ϕ=0.81 vs. ϕ=0.77. It is worth noting that these values are quite "penalized" by the high scatter of the experimental failure loads – high underestimations of the test results of Kwon & Hancock (1992) and equally high overestimations of the test results of Kwon *et al.* (2009), even if the overall mean value is above 1.0. If the test results reported by Kwon *et al.* (2009)[10] were to be removed, both approaches would perform better (particularly the NDL one): ϕ=0.85 vs. ϕ=0.78 – the former value now satisfies the NAS reliability demand for compression members (ϕ=0.85) – see Table 2.

(ii) Fig. 5(a)-(f) and 6(a)-(f) lead to a conclusion opposite to that drawn in the previous item: now the MNDL approach clearly outperforms its NDL counterpart. Indeed, the latter provides overly conservative estimates, as attested by the statistical indicators of P_U/P_{nDL} shown in those figures – note that the minimum value is very close to 1.0

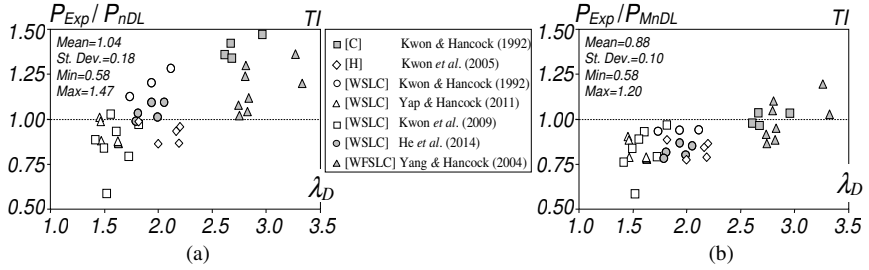

Fig. 4. Plots (a) P_{Exp}/P_{nDL} and (b) P_{Exp}/P_{MnDL} vs. λ_D concerning the available *experimental* failure loads for columns undergoing *true L-D interaction* (TI)

[10] In these tests, the specimen fixed-ended support conditions are a bit "suspicious", since they were achieved through a polyester resin capping system. The authors suspect that this arrangement is not capable of ensuring fully fixed-ended columns at advanced loading stages, making it logical to expect lower failure loads.

Table 2. LRFD resistance factors ϕ according to AISI (2012) concerning the *experimental* failure loads for columns undergoing *true L-D interaction* (TI) – NDL and MNDL approaches

Cross section	Reference		NDL			MNDL		
		n	P_m	V_p	ϕ	P_m	V_p	ϕ
C	Kwon & Hancock (1992)	4	1.40	0.06	1.20	1.00	0.04	0.90
H	Kwon *et al*. (2005)	5	0.92	0.05	0.82	0.83	0.05	0.75
WSLC	Kwon & Hancock (1992)	3	1.20	0.08	0.94	0.94	0.00	0.86
WSLC	Kwon *et al*. (2009)	7	0.86	0.13	0.69	0.82	0.13	0.66
WSLC	Yap & Hancock (2011)	6	0.91	0.07	0.81	0.82	0.06	0.73
WSLC	He *et al*. (2014)	14	1.01	0.09	0.88	0.84	0.04	0.77
WFSLC	Yang & Hancock (2004)	8	1.17	0.12	0.96	1.00	0.12	0.83
Total		47	1.04	0.18	0.81	0.88	0.10	0.77
Total excluding Kwon *et al*. (2009)		40	1.07	0.17	0.85	0.89	0.10	0.78

for all the columns. Once again, the resistance factors given in Table 3 confirm the above assertion: considering all columns, ϕ is equal to 1.03 and 0.93 for the NDL and MNDL approaches – both values fulfil the reliability target by a large margin.

(iii) Since the experimental and numerical failure load numbers are clearly "unbalanced" (47 vs. 1421), its is just logical that the joint consideration of both of them leads to resistance factors very similar to those obtained with the numerical failure loads.

(iv) Based on the contents of the previous items, it seems prudent, for the time being, to recommend the codification of the NDL approach to handle columns undergoing true L-D interaction (TI), even if it provides farly high underestimations of the numerical failure loads. This is because the resistance factor associated with the MNDL

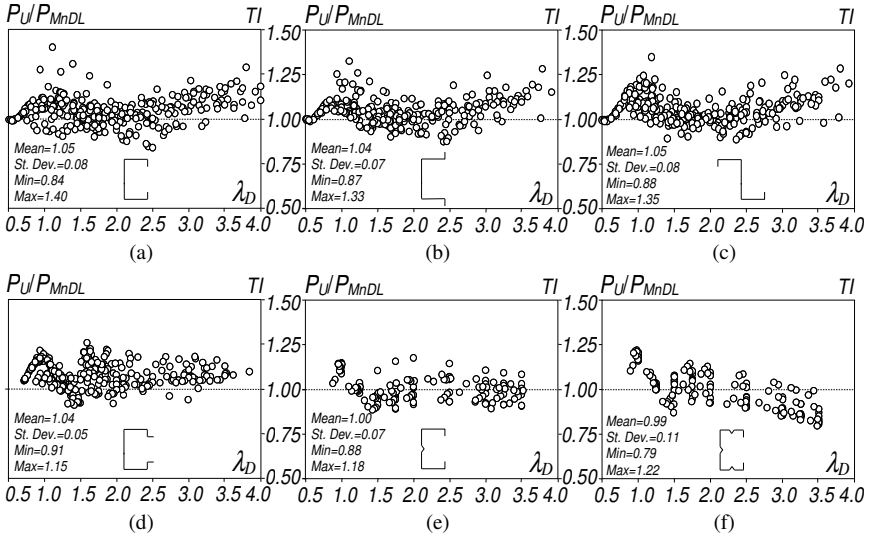

Fig. 5. Plots P_U/P_{MnDL} vs. λ_D concerning the *numerical* failure loads for columns undergoing *true L-D interaction* (TI): (a) C, (b) H, (c) Z, (d) R, (e) WSLC, (f) WFSLC columns

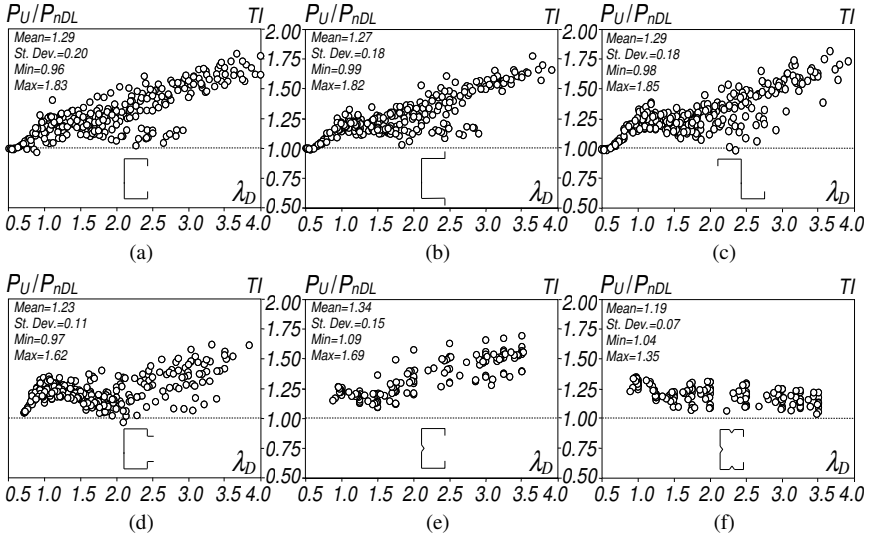

Fig. 6. Plots P_U/P_{nDL} vs. λ_D concerning the *numerical* failure loads for columns undergoing *true L-D interaction* (TI): (a) C, (b) H, (c) Z, (d) R, (e) WSLC, (f) WFSLC columns

Table 3. LRFD resistance factors ϕ according to AISI (2012) concerning the *numerical* failure loads of columns undergoing *true L-D interaction* (TI) – NDL and MNDL approaches

Cross section	Reference		NDL			MNDL		
		n	P_m	V_p	ϕ	P_m	V_p	ϕ
C	Dinis & Camotim (2015)	285	1.29	0.20	0.99	1.05	0.08	0.93
H	Silvestre *et al.* (2012)	269	1.27	0.18	1.01	1.04	0.07	0.94
Z	Silvestre *et al.* (2012)	279	1.29	0.18	1.02	1.05	0.08	0.94
R	Martins *et al.* (2015a)	304	1.23	0.11	1.06	1.08	0.07	0.97
WSLC	Martins *et al.* (2016a)	144	1.34	0.15	1.10	1.00	0.07	0.90
WFSLC	Martins *et al.* (2015b, 2016b)	140	1.19	0.07	1.07	0.99	0.11	0.86
Total		1421	1.27	0.16	1.03	1.04	0.08	0.93

approach falls below the prescribed ϕ=0.85 value. Nevertheless, it should be noted that this ϕ value is pratically equal to that obtained for the currently codified NL curve (ϕ=0.79 – see Schafer 2008)[11]. The authors believe that additional test results could raise the ϕ value obtained for the MNDL approach, bringing it closer to the prescribed one. If this happens, it may be possible to codify the MNDL approach (instead of the NDL one) to handle columns affected by TI, thus leading to more economic designs and, naturally, benefitting the CFS industry[12].

[11] The low resistance factor associated with the NL curve was "compensated" by considering jointly the local (ϕ=0.79) and distortional (ϕ=0.90) limit states, leading to a "combined" resistance factor ϕ=0.85 – see Schafer (2008). Since the authors feel that this "compensation" procedure is a bit "forced", a similar path was not followed in this work.

[12] A test campaign, to be carried out at The University of Hong Kong by Prof. Ben Young, is being planned.

3.2 Secondary Distortional Bifurcation L-D Interaction (SDI)

The SDI must also be taken into acount in the design of CFS columns (or any other members), due to their well known high local post-critical strength reserve. Naturally, any DSM-based approach intended to handle this type of L-D interaction should be, in one way or another, related to the current codified NL design curve. As a first step towards the development of such a design approach, it is essential to identify a "border" inside which L-D interaction becomes relevant. Based on the work reported by Martins *et al.* (2015a), a border of this nature may be defined (conservatively) by λ_L=0.85P_{crD}/P_{crL}, a condition depending on the values of P_{crD}, P_{crL}, P_y (dependence of the yield stress felt through λ_L) and establishing that (i) local failures occur for $\lambda_L \leq 0.85P_{crD}/P_{crL}$ and, conversely, (ii) L-D interactive failures occur for $\lambda_L > 0.85P_{crD}/P_{crL}$. Since the MNDL approach ceases to provide accurate estimates when P_{crD}/P_{crL} differs visibly from 1.0 (logical, since it was developed to handle TI) a novel DSM-based approach (NSDB) is sought. It is defined by (i) the NL design curve, for $\lambda_L \leq 0.85P_{crD}/P_{crL}$, (ii) by a "Winter-type" curve (unknown coefficients at this stage), for $\lambda_L \geq 0.85P_{crD}/P_{crL}+\Delta\lambda_L$, and, finally, (iii) a linear transition between the two previous curves (occurring in the $\Delta\lambda_L=\lambda_{L2}-\lambda_{L1}$ range) – the proposed approach, which is illustrated in Fig. 3(b), is defined by

$$P_{nSDB} = \begin{cases} P_{nL} & , \quad \lambda_L \leq \lambda_{L1} \\ P_1 + \dfrac{P_2 - P_1}{\lambda_{L2} - \lambda_{L1}}\left(\lambda_L - \lambda_{L1}\right), & \lambda_{L1} < \lambda_L < \lambda_{L2} \\ P_y \lambda_L^{-a}\left(1 - b\lambda_L^{-a}\right) & , \quad \lambda_L \geq \lambda_{L2} \end{cases} \tag{6}$$

where the various parameters (also indicated in Fig. 3(b)) are given by

$$\begin{gathered} P_1 = P_{y1}\lambda_{L1}^{-0.8}\left(1 - 0.15\lambda_{L1}^{-0.8}\right) \qquad P_2 = P_{y2}\lambda_{L2}^{-a}\left(1 - b\lambda_{L2}^{-a}\right) \\ \lambda_{L1} = m\frac{P_{crD}}{P_{crL}} \qquad \lambda_{L2} = \lambda_{L1} + \Delta\lambda_L \qquad P_{y1} = \lambda_{L1}^2 P_{crL} \qquad P_{y2} = \lambda_{L2}^2 P_{crL} \end{gathered} \tag{7}$$

The first estimate for the "Winter-type" curve parameters "a" and "b" was obtained by solving a minimization problem involving only the experimental failure load database (specimens undergoing SDI – see Table 1), aimed at reaching the reliability target. Then, the objective function is defined as

$$f(\boldsymbol{x}) = \sum_{i=1}^{N}\left(P_{U,i}^{Exp.} - P_{nSDB,i}(\boldsymbol{x})\right)^2 \tag{8}$$

which means that the (multivariable constraint) minimization problem becomes simply

$$\begin{gathered} min\ f(\boldsymbol{x}) \\ s.t.: \quad \phi \geq 0.85 \end{gathered} \tag{9}$$

where $\boldsymbol{x}$=[a,b] is a design variable vector and N is to the number of SDI specimens. As for $\Delta\lambda_L$, required to calculate the objective function, the evaluation of its value was based

on the numerical failure loads of columns experiencing SDI[13]: the value adopted was $\Delta\lambda_L$=0.25 – due to space limitations, no details on how this value was reached are given.

Table 4 gives the n, P_m, V_p and ϕ values for four different NSDB curves, *i.e.*, four pairs of (a,b) values. "Options 1 and 2" correspond to the solutions of the minimization problem defined by Eq. (9) – while the former is based on all experimental results, the latter excludes the results of Kwon *et al.* (2009) (reason mentioned earlier). "Options 3 and 4", which also exclude the results of Kwon *et al.* (2009), were developed to obtain a curve "more or less parallel" to the NDL one – see Fig. 3(b). Note that, since this curve is based on λ_{DL} (not λ_L), the coefficients in Eq. (1) (0.25, 1.20) are not equivalent to the pair (a,b) in Eq. (6). The observation of this table makes it possible to conclude that:

(i) "Option 1" shows that there exists an (a,b) pair that leads to accurate predictions of the experimental failure loads of columns affected by SDI, while fulfilling the reliability-based constraint.

(ii) Excluding the results of Kwon *et al*. (2009) ("Option 2") still improves the above solution, leading to P_m=1.016(>0.995), V_p=0.086(<0.122) and ϕ=0.90>0.85, which means that the prescribed ϕ value is outperformed.

(iii) As for the last two options, it is noted that "Option 3" satisfies the reliability demand, while "Option 4" fails to do so by a tiny margin but leads to more economic designs.

Table 4. LRFD resistance factors ϕ according to AISI (2012) concerning the *experimental* failure loads of column undergoing SDI and associated with four DSM–based design approaches

	Option 1	Option 2	Option 3	Option 4
a	1.267	1.248	1.25	1.20
b	0.338	0.340	0.15	0.15
n	64	56	56	56
P_m	0.995	1.016	0.976	0.959
V_p	0.122	0.086	0.101	0.108
ϕ	0.850	0.900	0.853	0.832

Finally, it remains to assess whether the NSDB approach just proposed ("Option 4") also predicts efficiently the numerical failure loads. Since Figs. 7(a)-(b) to 9(a)-(f)[14] and Tables 5-6 are similar to Figs. 4(a)-(b) to 6(a)-(f) and Tables 2-3, their descriptions are abbreviated here – the only difference is that the NSDB approach replaces the MNDL one. The observation of all these results prompts the following remarks:

(i) Figs. 8(a)-(f) immediately show that the NSDB approach can predict successfully the numerical failure loads associated with SDI. Indeed, the statistical indicators of the 670 failure loads given in Table 6 are excellent, both individually (for each cross-

[13] It is necessary to have several columns with the same P_{crD}/P_{crL} ratio and various yield stresses, *i.e.*, distinct local slenderness values – obviously, this requirement cannot be fulfilled with tested specimens (see Fig. 10(a)).

[14] The inclusion of the apparently "illogical" $P_{Exp}/P_{nSDB}(P_{nDL})$ vs. λ_D in the plots displayed in Figs. 8 and 9, instead of the more logical $P_{Exp}/P_{nSDB}(P_{nDL})$ vs. λ_L ones, was done to improve the readability, since those values were obtained by imposing several distortional slenderness values (λ_L=1.00, 1.25, 1.50, 1.75, 2.00, 2.50, 3.00, 3.25, 3.50), which means that they would be located on the same vertical line and, therefore, "on top of each other".

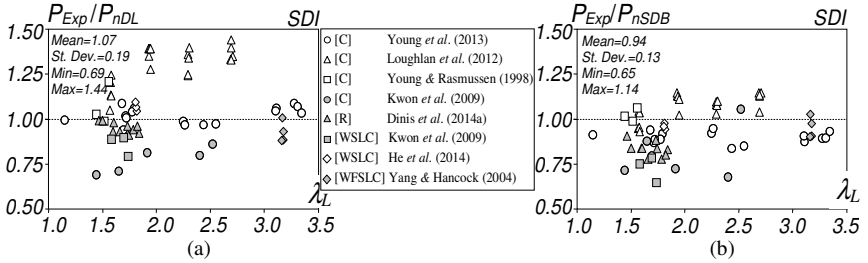

Fig. 7. Plots (a) P_{Exp}/P_{nDL} vs. λ_D and (b) P_{Exp}/P_{nSDB} vs. λ_D concerning the available *experimental* failure loads for columns undergoing *secondary distortional bifurcation L-D interaction* (SDI)

Table 5. LRFD resistance factors ϕ (AISI 2012) for the *experimental* failure loads of columns affected by *secondary distortional bifurcation L-D interaction* (SDI) – NDL and NSDB approaches

Cross section	Reference		NDL			NSDB		
		n	P_m	V_p	ϕ	P_m	V_p	ϕ
C	Young *et al*. (2013)	16	1.02	0.05	0.93	0.89	0.04	0.81
C	Loughlan *et al*. (2012)	20	1.30	0.11	1.12	1.07	0.07	0.96
C	Young &Rasmussen (1998)	3	1.07	0.12	0.72	1.02	0.04	0.91
C	Kwon *et al*. (2009)	5	0.77	0.07	0.67	0.81	0.16	0.58
R	Dinis *et al*. (2014a)	10	0.95	0.03	0.87	0.83	0.04	0.76
WSLC	Kwon *et al*. (2009)	3	0.86	0.06	0.72	0.73	0.16	0.40
WSLC	He *et al*. (2014)	3	1.07	0.03	0.97	0.96	0.02	0.88
WFSLC	Yang & Hancock (2004)	4	0.92	0.06	0.80	0.95	0.06	0.82
Total		64	1.07	0.19	0.83	0.94	0.13	0.80
Total excluding Kwon *et al*. (2009)		56	1.11	0.17	0.89	0.96	0.11	0.83

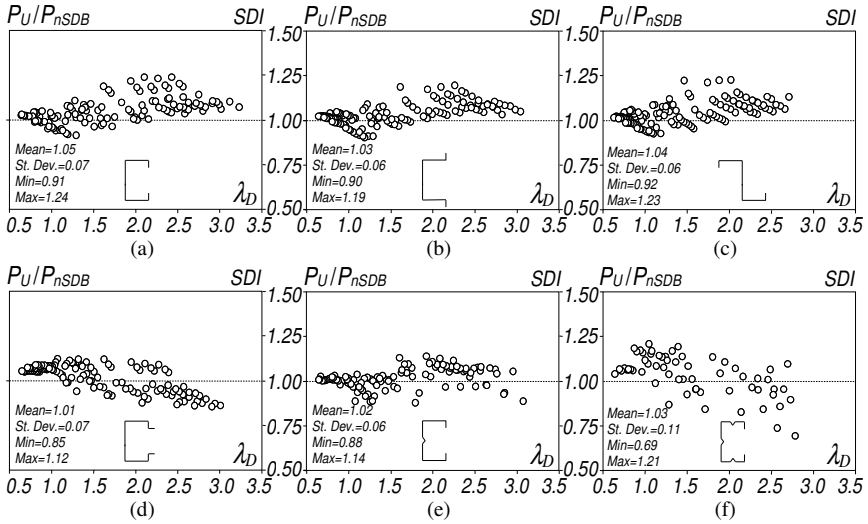

Fig. 8. Plots P_U/P_{nSDB} vs. λ_D for the *numerical* failure loads of columns undergoing *secondary distortional bifurcation L-D interaction* (SDI): (a) C, (b) H, (c) Z, (d) R, (e) WSLC, (f) WFSLC

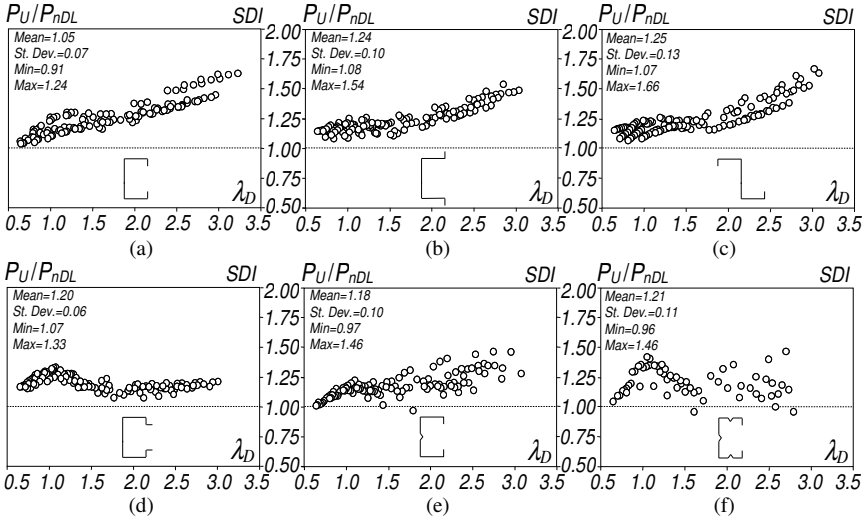

Fig. 9. Plots P_U/P_{nDL} vs. λ_D for the *numerical* failure loads of columns undergoing *secondary distortional bifurcation L-D interaction* (SDI): (a) C, (b) H, (c) Z, (d) R, (e) WSLC, (f) WFSLC

Table 6. LRFD resistance factors ϕ (AISI 2012) for the *numerical* failure loads of columns affected by *secondary distortional bifurcation L-D interaction* (SDI) – NDL and NSDB approaches

Cross section	Reference		NDL			NSDB		
		n	P_m	V_p	ϕ	P_m	V_p	ϕ
C	Martins *et al*. (2015a)	120	1.26	0.14	1.06	1.05	0.07	0.95
H		130	1.24	0.10	1.08	1.03	0.06	0.94
Z		130	1.25	0.13	1.06	1.04	0.06	0.94
R		120	1.20	0.06	1.09	1.01	0.07	0.91
WSLC	Martins *et al*. (2016a)	108	1.18	0.10	1.03	1.02	0.06	0.92
WFSLC	Martins *et al*. (2015b, 2016b)	62	1.21	0.11	1.04	1.03	0.11	0.89
Total		670	1.22	0.11	1.06	1.03	0.07	0.93

section type) and combined – in the latter case, the mean and standard deviation are equal to 1.03 and 0.07, respectively, leading to ϕ=0.93>0.85. On the other hand, the NDL approach provides once again conservative results: P_m=1.22, V_p=0.11 and ϕ=1.06>0.93 – see Figs. 9(a)-(f) and Table 6. In order to make it clear that the NSDB approach predicts efficiently the numerical failure data, in spite of the fact that it was developed on the basis of experimental failure loads, Figs. 10(a_1)-(a_2) plot P_{nSDB}/P_y vs. λ_L for 18 Z-columns (b_w=120, b_f=100, b_l=10 and L=1000mm – see Fig. 1) with several yields stresses (λ_L values): (i_1) 9 for a column with P_{crD}/P_{crL}=1.5 (t=1.15mm – Fig. 10(a_1)) and (i_2) 9 for a column with P_{crD}/P_{crL}=2.0 (t=0.70mm – Fig. 10(a_2)). Note that, obviously, the NSDB approach depends on the P_{crD}/P_{crL} value. In addition, Figs. 10(b_1)-(b_2) show the failure modes of the Z+λ_L=1.5 (local) and Z+λ_L=3.0 (L-D interactive) columns. These figures "illustrate" graphically the above assertion.

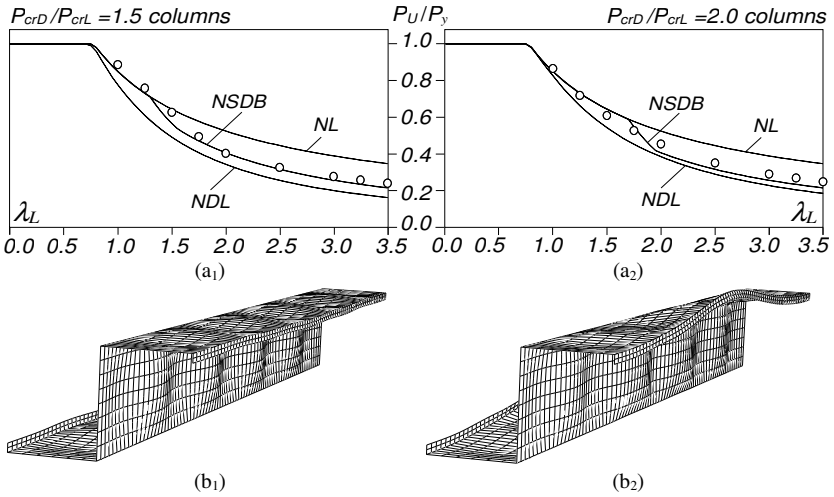

Fig. 10. Plots of P_{nSDB}/P_y vs. λ_L for Z-columns with λ_L={1.00, 1.25, 1.50, 1.75, 2.00, 2.50, 3.00, 3.25, 3.50}, P_{crD}/P_{crL} equal to (a_1) 1.5, (a_2) 2.0 and (b) failure modes for (b_1) Z+λ_L=1.5 and (b_2) Z+λ_L=3.0

(ii) The joint observation of Figs. 7(a)-(b) and Table 5 shows that the P_{Exp}/P_{nDL} values exhibit higher means and are more scattered than their P_{Exp}/P_{nSDB} counterparts. Nevertheless, however, there no significant difference between the corresponding resistance factors – ϕ=0.83 vs. ϕ=0.80 or ϕ=0.89 vs. ϕ=0.83, depending on whether the results reported by Kwon *et al.* (2009) are considered or not.

(iii) It seems clear that the NSDB approach is the most adequate design proposal to account for the SBI effects, since it exhibits reasonably good statistical indicators for both the experimental and numerical failure loads, while leading to more economic designs than the NDL approach – see Fig. 3(b).

3.3 Secondary Local Bifurcation L-D Interaction (SLI)

Numerical results recently reported by the authors (Martins *et al.* 2015a) showed that SLI causes only negligible failure load erosion with respect to the ultimate strength provided by the currently codified distortional design curve (ND). The moderate distortional post-critical distortional strength reserve (when compared with its local counterpart) precludes the occurrence of significant L-D interaction even for very high yield stresses. Like in the SDI case, addressed in Section 3.2, it is possible to think of a "border" separating the columns failing in (i) distortional and (ii) L-D interactive modes – based on the study of Martins *et al.* (2015a), such border may be conservatively defined by λ_D=3.5P_{crD}/P_{crL}[15]. In order to assess the validity of this assertion, Figs. 11(a)-(b) plot P_{Exp}/P_{nD} vs. λ_D for the failure loads of tested specimens undergoing SLI and provide the corresponding n, P_m, V_p, ϕ values associated with the DSM distortional strength predictions (P_{nD}). On the other

[15] Like its SDI counterpart, this condition depends on the values of P_{crD}, P_{crL}, P_y.

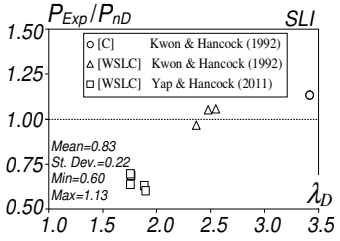

(a)

Cross section	Reference	n	ND P_m	ND V_p	ND ϕ
C	Kwon & Hancock (1992)	1	1.13	0.00	1.05
WSLC	Kwon & Hancock (1992)	3	1.03	0.05	0.88
WSLC	Yap & Hancock (2011)	5	0.65	0.04	0.59
Total		9	0.83	0.22	0.57

(b)

Fig. 11. (a) Plots P_{Exp}/P_{nD} vs. λ_D for the available *experimental* failure loads of columns undergoing *secondary local bifurcation L-D interaction* (SLI) and (b) LRFD resistance factors ϕ (AISI 2012)

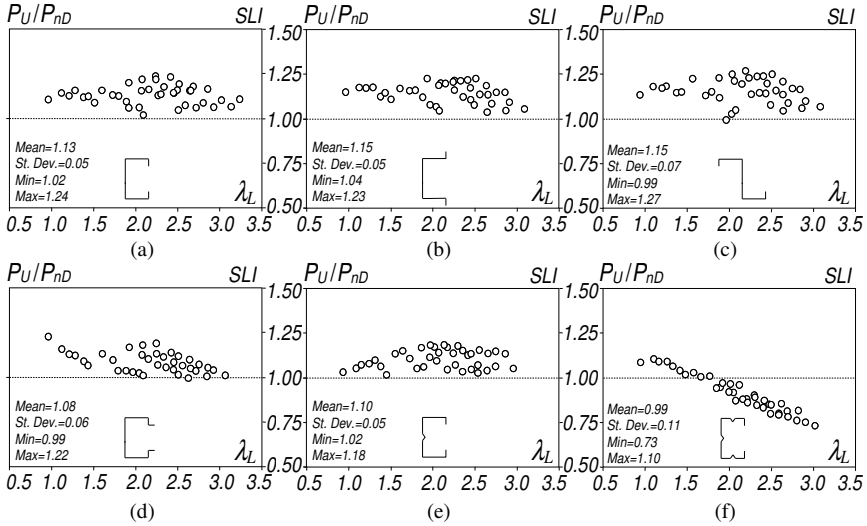

(a) (b) (c)

(d) (e) (f)

Fig. 12. Plots P_U/P_{nD} vs. λ_L for the available *numerical* results failure loads of columns undergoing *secondary local bifurcation L-D interaction* (SLI): (a) C, (b) H, (c) Z, (d) R, (e) WSLC, (f) WFSLC

Table 7. LRFD resistance factors ϕ according to AISI (2012) for the *numerical* failure loads of columns affected by *secondary local bifurcation L-D interaction* (SLI) – ND approach

Cross section	Reference	n	ND P_m	ND V_p	ND ϕ
C	Martins *et al*. (2015a)	40	1.13	0.05	1.03
H		38	1.15	0.05	1.04
Z		37	1.15	0.07	1.04
R		37	1.08	0.06	0.98
WSLC	Martins *et al*. (2016a)	38	1.10	0.05	1.00
WFSLC	Martins *et al*. (2015b, 2016b)	38	0.91	0.11	0.79
Total		191	1.09	0.11	0.94

hand, Figs. 12(a)-(f), similar to Figs. 5-6 and 8-9 presented in Sections 3.1 and 3.2, show plots P_U/P_{nD} vs. λ_L[16], concerning the available numerical failure loads, and Table 7 provides the corresponding statistical indicators. The observation of all these results prompts the following comments:

(i) Although the amount of experimental failure loads of columns undergoing SLI is very scarce, Fig. 11(a) shows a huge disparity between two set of results. Indeed, while the failure loads of the four specimens tested by Kwon & Hancock (1992), concerning one C and three WSLC columns, are adequately (safely and accurately) predicted by the currently codified distortional design curve, those exhibited by the five WSLC column specimens tested by Yap & Hancock (2011) are heavily overestimated by that same curve[17]. Although the authors have no clear explanation for this large and surprising discrepancy, it should be noted that a similar (but less pronounced) trend was observed for the 3 specimen tests reported by Yap (2008), which have the same cross-section as those included in Table 1 and failed in local modes: mean and standard deviation of the three P_{Exp}/P_{nL} values equal 0.79 and 0.06, respectively. In addition, this same overestimation tendency was also observed in the column specimens tested by this author and undergoing TI and SDI (see Table 1). The fact that the failure loads obtained in the tests reported by Yap (2008) and Yap & Hancock (2011) are systematically below the expected values seems to indicate that either (i_1) the authors of this paper have misinterpreted the test data or (i_2) some features of the test set-up and procedure were not adequately reported or achieved as planned (*e.g.*, the test set-up may not have ensured fully fixed end conditions).

(ii) As expected, the performance of the ND curve in predicting the numerical failures loads is much better – indeed, the P_U/P_{nD} value mean and standard deviation are equal 1.09 and 0.11, leading to a resistance factor ϕ=0.94>0.85. However, while the C, H, Z, R, WSLC columns P_U/P_{nD} values exhibit similar "clouds" (along λ_L), those concerning the WFSLC column are clearly different: they decrease faster with λ_L and fall below 1.0 for λ_L>2.0, which is due to the lower distortional post-critical strength reserve, particularly in the high slenderness range (Martins *et al*. 2015b) – therefore, the resistance factor obtained (ϕ=0.79) is a bit low, due to the inevitable high scatter.

3.4 Summary and Proposals

On the basis of the results and findings reported in Sections 3.1 to 3.3, it is now possible to propose DSM-based design approaches to predict the failure loads of CFS columns experiencing L-D interaction. At this stage it is worth mentioning that these proposals are made disregarding a few test results providing failure loads much lower than expected on the basis of other test results and numerical simulations, namely (i) three tests of by Kwon *et al.* (2009) (SDI) and (ii) five tests of Yap & Hancock (2011) (SLI).

[16] See Footnote 14, now applied to λ_D.

[17] Although hardly meaningful, due to the minute sample sizes, the LRFD resistance factors associated with the three sets of tested specimens indicated in Fig. 11(b), which are (i) ϕ=1.05 and ϕ=0.88, for the tests of Kwon & Hancock (1992), and (ii) ϕ=0.59, for the tests of Yap & Hancock (2011), clearly reflect the above huge disparity.

Since it was concluded that the failure loads of columns undergoing SLI (*i.e.*, such that $P_{crD}/P_{crL}<0.8$) can be adequately predicted by the currently codified DSM distortional strength curve, this same curve is proposed to handle such columns.

Concerning the prediction of the failure loads of columns experiencing TI or SDI ($0.8 \leq P_{crD}/P_{crL} \leq 1.3$ and $P_{crD}/P_{crL}>1.3$, respectively), it is possible to propose a joint DSM-based design approach, combining the available NDL approach for columns undergoing TI with the NSDB one ("Option 4") for columns undergoing SDI (see Section 3.2), which is termed "NLD approach"[18] and defined by

$$P_{nLD} = \begin{cases} 0.80 \leq \dfrac{P_{\mathrm{crD}}}{P_{\mathrm{crL}}} \leq 1.30, & \begin{cases} P_{nL} & , \quad \lambda_{DL} \leq 0.561 \\ P_{nL}\lambda_{DL}^{-1.2}(1-0.25\lambda_{DL}^{-1.2}) & , \quad \lambda_{DL} > 0.561 \end{cases} \\ \dfrac{P_{\mathrm{crD}}}{P_{\mathrm{crL}}} \geq 1.30, & \begin{cases} P_{nL} & , \quad \lambda_L \leq 0.85\dfrac{P_{crD}}{P_{crL}} \\ P_1 + \dfrac{P_2 - P_1}{0.25}\left(\lambda_L - 0.85\dfrac{P_{crD}}{P_{crL}}\right), & 0.85\dfrac{P_{crD}}{P_{crL}} < \lambda_L < 0.85\dfrac{P_{crD}}{P_{crL}} + 0.25 \\ P_y\lambda_L^{-1.2}\left(1-0.15\lambda_L^{-1.2}\right) & , \quad \lambda_L \geq 0.85\dfrac{P_{crD}}{P_{crL}} + 0.25 \end{cases} \end{cases} \tag{10}$$

4. Conclusion

This paper presented and discussed proposals for the codification of efficient design approaches for cold-formed steel columns affected by L-D interaction. These DSM-based proposals were developed, calibrated and validated on the basis of experimental and numerical failure load data reported by various researchers and concerning columns with several cross-section shapes, namely plain, web-stiffened and web/flange-stiffened lipped channels, hat-sections, zed-sections and rack-sections. Three types of L-D interaction were taken into account: true L-D interaction (TI), secondary distortional bifurcation L-D interaction (SDI) and secondary local bifurcation L-D interaction (SLI) – the classification depends on the ratio between the critical distortional and local buckling loads (P_{crD}/P_{crL}). In addition, the existing DSM-based design approaches to handle column L-D interactive failures were reviewed and their merits were assessed and compared with those of the proposed ones. Finally, the paper also presented reliability assessments of the failure load predictions provided by the proposed DSM-based design approaches, following the procedure prescribed by the North American Specification (AISI 2012).

After collecting the available experimental and numerical failure load data concerning columns affected by each of the three types of L-D interaction, the paper addressed the existing DSM-based approaches to handle this coupling phenomenon, and also presented the formula prescribed in AISI (2012) to evaluate the LRFD resistance factor ϕ.

Concerning columns undergoing TI, two DSM-based approaches (NDL and MNDL) were assessed and opposite conclusions were obtained for the experimental and numerical

[18] Do not confuse with the existing DSM design approach, defined in Eq. (2).

data: while NDL predicts satisfactorily the experimental data but heavily underestimates the numerical ones, MNDL provides excellent predictions of the numerical data but clearly overestimates several experimental failure loads. In order to ensure a resistance factor such that $\phi \geq 0.85$, it was decided to propose the NDL approach. However, the authors believe that additional experimental data are likely to enable the codification of the MNDL approach, which leads to more economic designs (higher strengths) and, therefore, benefits the CFS industry – a test campaign is planned for the near future.

Concerning columns undergoing SDI, a novel DSM-based approach was (i) developed, on the basis of the available experimental data, and subsequently, (ii) verified against the numerical data. It is termed NSDB approach and depends on P_{crD}/P_{crL} and λ_L (the key parameters influencing this coupling phenomenon): its proposal is based on the fact that it outperforms the NDL approach in predicting both the experimental and numerical data.

Finally, it was concluded that the failure loads of columns undergoing SDI can be adequately predicted by the currently codified distortional design curve, since the ultimate strength erosion, with the respect to that curve, was found to be negligible.

Acknowledgements

The first author gratefully acknowledges the financial support of FCT (*Fundação para a Ciência e a Tecnologia* – Portugal) – doctoral scholarship SFRH/BD/87746/2012.

References

American Iron and Steel Institute (AISI) (2012). *North American Specification* (NAS) *for the Design of Cold-Formed Steel Structural Members* (AISI-S100-12), Washington DC.

Bebiano R, Pina P, Silvestre N, Camotim D (2008). *GBTUL 1.0β – Buckling and Vibration Analysis of Thin-Walled Members*, DECivil/IST, Technical University of Lisbon.

Dinis PB, Young B, Camotim D (2014a). Local-distortional interaction in cold-formed steel rack-section columns, *Thin-Walled Structures*, **81**(August), 185-194.

Dinis PB, Young B, Camotim D (2014b). Strength, interactive failure and design of web-stiffened lipped channel columns exhibiting distortional buckling, *Thin-Walled Structures*, **81**(August), 195-209.

Dinis PB, Camotim D (2015). Cold-formed steel columns undergoing local-distortional coupling: behaviour and direct strength prediction against interactive failure, *Computers & Structures*, **147**(January), 181-208.

He Z, Zhou X, Liu Z, Chen M (2014). Post-buckling behaviour and DSM design of web-stiffened lipped channel columns with distortional and local mode interaction, *Thin-Walled Structures,* **84**(November), 189-203.

Kwon YB, Hancock GJ (1992). Tests of cold-formed channels with local and distortional buckling, *Journal of Structural Engineering* (ASCE)*,* **118**(7), 1786-1803.

Kwon YB*,* Kim BS, Hancock GJ (2009). Compression tests of high strength cold-formed steel channel with buckling interaction, *Journal of Constructional Steel Research,* **65**(2), 278-289.

Kwon YB, Kim NK, Kim BS (2005). A study on the direct strength method for compression members undergoing mixed mode buckling, *Proceedings of Third International Symposium on Steel Structures* (ISSS'05 – Seoul 10-11/03), 108-119.

Loughlan J, Yidris N, Jones K (2012). The failure of thin-walled lipped channel compression members due to coupled local-distortional interactions and material yielding, *Thin-Walled Structures,* **61**(December), 14-21.

Martins AD, Dinis PB, Camotim D, Providência P (2015a). On the relevance of local-distortional interaction effects in the behaviour and design of cold-formed steel columns, *Computers & Structures*, **160**(November), 57-89.

Martins AD, Dinis PB, Camotim D, Providência P (2015b). On the influence of local-distortional interaction effects in the behaviour and design of stiffened cold-formed steel columns, *CD-ROM Proceedings of Eighth International Conference on Advances in Steel Structures* (ICASS 2015, Lisbon, 21-24/7), paper 37.

Martins AD, Dinis PB, Camotim D (2016a). On the influence of local-distortional interaction in the behaviour and design of cold-formed steel web-stiffened lipped channel columns, *Thin-Walled Structures*, **101**(April), 181-204.

Martins AD, Camotim D, Dinis PB (2016b). Behaviour and DSM design of cold-formed steel stiffened lipped channel columns undergoing local-distortional interaction, *submitted for publication.*

Schafer BW, Peköz T (1998). Computational modeling of cold-formed steel: characterizing geometric imperfections and residual stresses, *Journal of Constructional Steel Research,* **47**(3), 193-210.

Schafer BW (2002). Local, distortional and Euler buckling in thin-walled columns, *Journal of Structural Engineering* (ASCE)*,* **128**(3), 289-299.

Schafer BW (2008). Review: the direct strength method of cold-formed steel member design, *Journal of Constructional Steel Research,* **64**(7-8), 766-778.

Simulia Inc. (2008), *ABAQUS Standard* (version 6.7-5).

Silvestre N, Camotim D, Dinis PB (2012). Post-buckling behaviour and direct strength design of lipped channel columns experiencing local/distortional interaction, *Journal of Constructional Steel Research,* **73**(June), 12-30.

Yang D, Hancock GJ (2004). Compression tests of high strength steel channel columns with interaction between local and distortional buckling, *Journal of Structural Engineering* (ASCE)*,* **130**(12), 1954-1963.

Yap DCY (2008). *Local and Distortional Buckling of High Strength Cold-Formed Steel Sections*, Ph.D. Thesis, School of Civil Engineering, University of Sydney, Australia.

Yap DCY, Hancock GJ (2011). Experimental study of high strength cold-formed stiffened-web C-sections in compression, *Journal of Structural Engineering* (ASCE)*,* **137**(2), 162-172.

Yap DCY, Hancock GJ (2008). Experimental study of complex high-strength cold-formed cross-shaped steel section, *Journal of Structural Engineering* (ASCE)*,* **134**(8), 1322-1333.

Young B, Rasmussen KJR (1998). Design of lipped channel columns, *Journal of Structural Engineering* (ASCE)*,* **124**(2), 140-148.

Young B, Silvestre N, Camotim D (2013). Cold-formed steel lipped channel columns influenced by local-distortional interaction: strength and DSM design, *Journal of Structural Engineering* (ASCE)*,* **139**(6), 1059-1074.